

# Physics programme of ALICE 3: A next-generation heavy-ion detector for LHC Run 5 and beyond

Nicola Nicassio<sup>1,\*</sup>, on behalf of the ALICE Collaboration

<sup>1</sup>Dipartimento Interateneo di Fisica ‘M. Merlin’ and Sezione INFN, Via Orabona 4, Bari, Italy

**Abstract.** The ALICE Collaboration is designing a completely new apparatus, ALICE 3, for the LHC Runs 5 and 6. The detector comprises a large pixel-based tracking system covering eight units of pseudorapidity, complemented by various particle identification systems including silicon time-of-flight layers, a ring-imaging Cherenkov detector, a muon identification system, an electromagnetic calorimeter and a forward conversion tracker. ALICE 3 will, on the one hand, enable novel studies of the quark-gluon plasma (QGP) and, on the other hand, open up important physics opportunities in other areas of QCD and beyond. The main new studies in the QGP sector focus on low- $p_T$  heavy-flavour production, including beauty hadrons, multi-charm baryons and charm-charm correlations, as well as on precise multi-differential measurements of dielectrons to probe the mechanism of chiral-symmetry restoration and the time-evolution of the QGP temperature. Besides QGP studies, ALICE 3 can uniquely contribute to hadronic physics, with femtoscopic studies of the interaction potentials between charm mesons and searches for nuclei with charm, and to fundamental physics, with tests of the Low theorem for ultra-soft photon emission. This contribution will cover the latest detector concept and the state-of-the-art projections for the resulting physics performance in dielectron and heavy-flavour measurements.

## 1 Introduction

ALICE (A Large Ion Collider Experiment) is a general-purpose experiment at the CERN LHC designed to study the microscopic dynamics of the strongly interacting matter produced in heavy-ion collisions and, in particular, the quark-gluon plasma (QGP), a state of matter where quarks and gluons are deconfined. The LHC Runs 1 and 2 led to significant advances in our understanding of the QCD phase diagram and of the QGP [1]. With the current major upgrade to ALICE 2 and the future upgrade to ALICE 2.1, which will see an upgrade of the inner silicon tracker layers (ITS3) and a new system of forward electromagnetic and hadronic calorimeters (FoCal), LHC Runs 3 and 4 will enable further systematic measurements of fundamental properties for our understanding of the QGP [2]. However, despite the rich planned physics programme, fundamental questions will remain open, such as the QGP properties driving its constituents to equilibration, the hadronization mechanisms of the medium, the partonic equation of state and its temperature dependence, and the underlying dynamics of chiral symmetry restoration. Addressing such questions requires substantial improvements in terms of detector performance and rate capabilities, calling for a next-generation experiment, ALICE 3, planned for LHC Run 5 and beyond [3].

\*e-mail: [Nicola.Nicassio@ba.infn.it](mailto:Nicola.Nicassio@ba.infn.it)

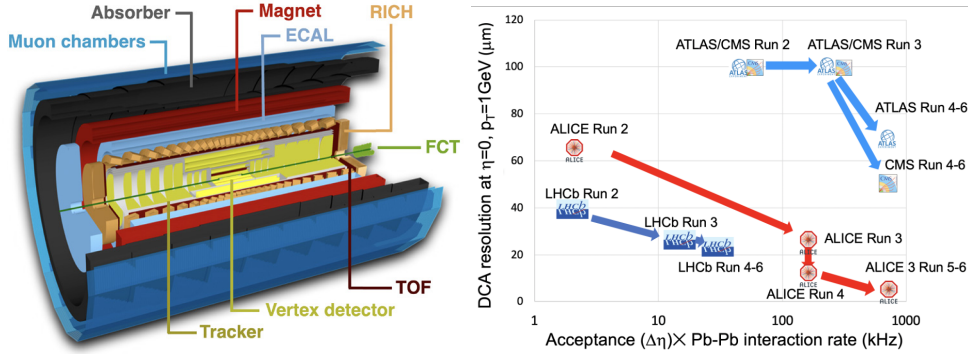


**Figure 1.** Left: ALICE 3 state-of-the-art detector concept. Right: Improvement of ALICE pointing resolution and expected effective statistics in Pb-Pb collisions from Run 2 to Run 6 compared with LHCb, CMS and ATLAS current projections.

## 2 ALICE 3 physics goals

The ALICE 3 primary goal is the understanding of the mechanisms ruling the different stages of heavy-ion collisions, from the medium formation to the heavy-flavour diffusion, thermalization and hadronization in the QGP. The ALICE 3 design is optimized for measurements of low transverse momentum ( $p_T$ ) heavy-flavour production, including charm-charm correlations, multi-charm baryon and beauty hadron production, as well as measurements of net-quantum number fluctuations to constrain the susceptibilities of the QGP and dileptons to probe the time-evolution of the QGP and the mechanism of chiral symmetry restoration in the medium. Besides QGP studies, ALICE 3 can uniquely contribute to hadronic physics, with femtoscopic studies of the interaction potentials between charm mesons and searches for nuclei with charm. ALICE 3 can also contribute to fundamental physics, with precision experimental tests of Low's theorem for ultra-soft photon emission and searches for axion-like particles in ultra-peripheral heavy-ion collisions via light-by-light scattering measurements.

## 3 ALICE 3 detector concept

All the measurements outlined in Sect. 2 set requirements on vertexing, tracking, particle identification and rate capabilities. The combination of these requirements led to the state-of-the-art detector concept sketched in the left panel of Fig. 1. The key requirements are a retractable vertex detector featuring an unprecedented pointing resolution, a compact and lightweight all-silicon tracker embedded in a superconducting solenoidal magnet, efficient identification of  $\gamma$ ,  $e^\pm$ ,  $\mu^\pm$ ,  $\pi^\pm$ ,  $K^\pm$ ,  $p$  and  $\bar{p}$ , acceptance over eight units of pseudorapidity ( $|\eta| < 4$ ) and forward subsystems for event characterisation as well as continuous read-out combined with online data processing. The uniqueness of ALICE 3 in terms of pointing resolution and effective statistics is demonstrated in the right panel of Fig. 1, which shows the corresponding expected improvement by order of magnitudes from ALICE 2 (Run 2) to ALICE 3 (Runs 5 and 6) compared with LHCb, CMS and ATLAS current projections.

The heart of ALICE 3 is a retractable vertex detector made of three layers in the barrel and three disks at each end-cap based on curved wafer-scaled ultra-thin silicon Monolithic Active Pixel Sensors (MAPS) sensors installed in secondary vacuum inside the beampipe with the inner layer placed at 5 mm distance from the beam line after beam stabilisation. The resulting pointing resolution for pions at  $\eta = 0$  is shown as a function of  $p_T$  in the left panel of Fig. 2. A pointing resolution better than  $10 \mu\text{m}$  is ensured for  $p_T$  larger than 200 MeV.

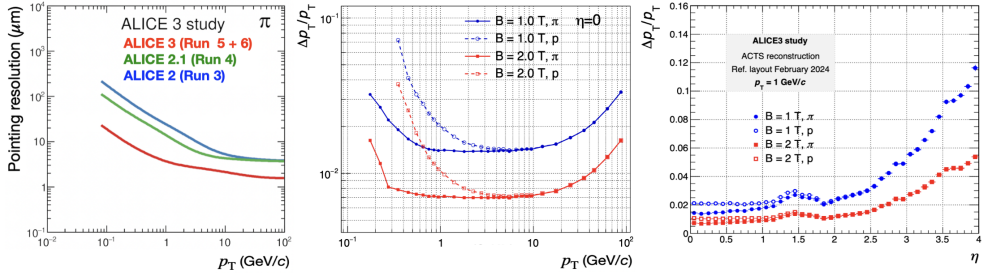


**Figure 2.** Left: Pointing resolution for pions as a function of  $p_T$ . Middle and right: Relative  $p_T$  resolution for pions and protons as a function of both  $p_T$  and  $\eta$  assuming  $B = 1$  T and  $B = 2$  T.

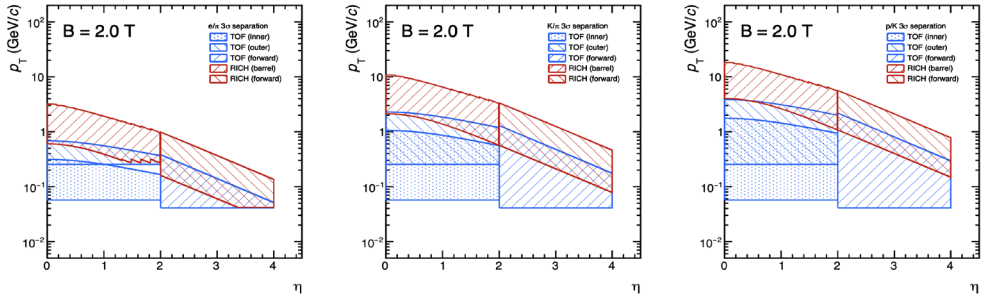


**Figure 3.** Expected  $\eta$ - $p_T$  regions with larger than  $3\sigma$  separation using ALICE 3 TOF and RICH systems for  $B = 2$  T. Electron/pion, pion/kaon and kaon proton separation plots are shown from left to right.

The ALICE 3 tracking system consists of eight cylindrical layers and nine forward disks at each end-cap equipped with MAPS installed in a volume of 7 m length and 80 cm radius. The middle and right panels of Fig. 2 show the resulting relative  $p_T$  resolution for pions and protons as a function of  $p_T$  at  $\eta = 0$  and as a function of  $\eta$  at  $p_T = 1$  GeV/c. The curves obtained assuming a magnetic field of  $B = 1$  T and  $B = 2$  T are compared, with  $B = 2$  T being the baseline. A better than 2% relative  $p_T$  resolution is ensured over a wide  $\eta$  range.

The particle identification system consists of Time-of-Flight (TOF) and Ring-Imaging Cherenkov (RICH) subsystems, an electromagnetic calorimeter (ECAL), a Muon Identification system (MID) and a Forward Conversion Tracker (FCT). With a time resolution of 20 ps, an inner TOF layer at 19 cm radius (iTOF), an outer layer at 85 cm radius (oTOF) and forward disks at  $\pm 3.70$  m distance from the interaction point (fTOF), better than  $3\sigma$   $e/\pi$ ,  $\pi/K$  and  $K/p$  separation is achieved up to 0.7, 2 and 4 GeV/c momentum, respectively. Low Gain Avalanche Diodes (LGADs), both hybrid and monolithic in CMOS technology, and Silicon Photomultipliers (SiPMs) are under study as viable technology options for the TOF sensors. The oTOF and fTOF are followed by a projective barrel RICH layer (bRICH) and forward RICH disks (fRICH). With aerogel as Cherenkov radiator and a SiPM-based photodetector in a proximity-focusing configuration, the RICH extends the  $3\sigma$   $e/\pi$ ,  $\pi/K$  and  $K/p$  separation up to 3, 10 and 17 GeV/c momentum, respectively. The resulting TOF and RICH particle identification coverage in the  $\eta$ - $p_T$  plane is shown in Fig. 3. The ECAL, MID and the FCT are designed to provide identification of high-energy photons and electrons up to hundreds of GeV for  $-4 < \eta < 1.5$ , muons down to  $p_T \approx 1.5$  GeV/c for  $|\eta| < 1.3$  and soft photons with  $p_T$  down to 1 MeV/c for  $4 < \eta < 5$ , respectively. The ECAL is based on Pb-scintillator sampling technology and includes a high-energy resolution segment based on PbWO<sub>4</sub> crystals at  $\eta = 0$  with SiPM readout. The MID consists of a steel hadron absorber followed by dedicated muon chambers made of scintillator bars readout using SiPMs. Alternative options based on Multi-Wire Proportional Chambers (MWPCs) and Resistive Plate Chambers (RPCs) are also under study. Finally, the FCT consists of forward disks equipped with MAPS.

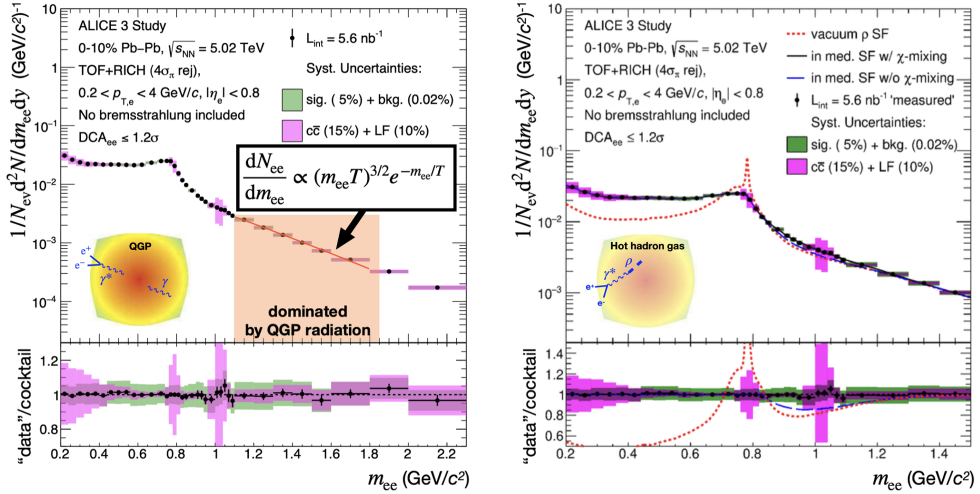


**Figure 4.** Simulated background-subtracted dielectron invariant mass spectrum in central (0-10%) Pb-Pb collisions at  $\sqrt{s_{NN}} = 5.02$  TeV. Left: Fit of the spectrum with an exponential model in the  $m_{ee}$  range 1.1-1.8  $\text{GeV}/c^2$  to extract the early-stage QGP temperature. Right: Comparison of the spectrum obtained using the  $\rho$  spectral function in medium under the hypothesis of  $\rho$ - $a_1$  mixing with expectations for the  $\rho$  spectral function in vacuum and in medium without chiral mixing.

## 4 ALICE 3 physics performance

In this section, a selection of simulations on the expected ALICE 3 physics performance is reported highlighting the impact of each subsystem specifications on the physics programme. The projections take into account that, throughout LHC Runs 5 and 6, ALICE 3 will collect integrated luminosities of  $18 \text{ fb}^{-1}$  and  $35 \text{ nb}^{-1}$  for pp and Pb-Pb collisions, respectively.

### 4.1 Dielectrons

Dileptons are produced in all the different stages of a heavy-ion collision. Since they are not interacting via the strong force, they leave the collision unscattered after production, making them ideal messengers to study the whole evolution of the collision [4]. Fig. 4 shows the the ALICE 3 projection for the expected background-subtracted thermal dielectron invariant mass ( $m_{ee}$ ) spectrum for central Pb-Pb collisions at center-of-mass energy per nucleon pair  $\sqrt{s_{NN}} = 5.02$  TeV. In the region above 1  $\text{GeV}/c^2$ , the slope of the spectrum provides direct information on the QGP temperature, as shown in the left panel of Fig. 4. With the very large expected statistics, ALICE 3 will also open up the possibility of probing the time dependence of QGP temperature using double differential dilepton spectra of  $m_{ee}$  and dielectron transverse momentum  $p_{T,ee}$ . For  $m_{ee} < 1.2 \text{ GeV}/c^2$ , the shape of the spectrum is dominated by thermal production of  $\rho$  mesons. Their spectral function (SF) is modified in the hot medium where chiral symmetry restoration is predicted. The expected high-precision measurement of the  $m_{ee}$  spectrum in central Pb-Pb collision with ALICE 3 would enable the study of chiral symmetry restoration mechanisms like  $\rho$ - $a_1$  mixing [5], as shown in the right panel of Fig. 4. The key ALICE 3 ingredients to achieve the desired statistical and systematic precision are the excellent  $e^\pm$  identification down to low  $p_T$  achieved with TOF and RICH, the small detector material budget to reduce the combinatorial background from  $\gamma$  conversion or  $\pi^0$  Dalitz decays and the excellent pointing resolution to efficiently suppress the dominant background from heavy-flavour hadron decays.

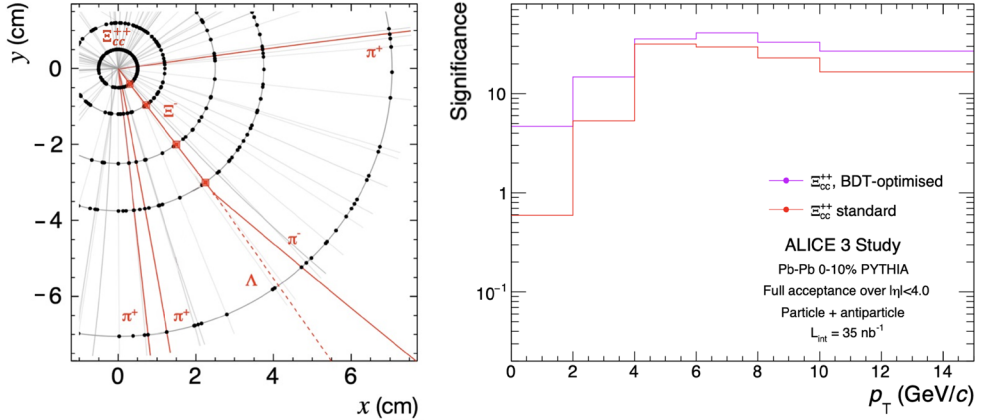


**Figure 5.** Left: ALICE 3 strangeness tracking in  $\Xi_{cc}^{++} \rightarrow \Xi_c^+ + \pi^+$  with  $\Xi_c^+ \rightarrow \Xi^- + 2\pi^+$ . Right: Simulated  $\Xi_{cc}^{++}$  significance in central (0-10%) Pb-Pb collisions at  $\sqrt{s_{NN}} = 5.52$  TeV as a function of  $p_T$  using standard selections (lower curve) and machine learning (upper curve).

## 4.2 Multi-charm baryons

Multi-charm baryon yields are powerful probes of the hadron formation mechanisms since they are expected to be produced through combination of uncorrelated charm produced in heavy-ion collisions [6]. ALICE 3 will enable systematic measurements of multi-charm states currently inaccessible, such as  $\Xi_{cc}^{++}$  through decay to  $\Xi_c^+ \pi^+$  with the subsequent decay  $\Xi_c^+ \rightarrow \Xi^- \pi^+ \pi^+$ . With the first tracking layer at 5 mm from the beam axis, strange baryons like  $\Xi^-$  can be directly tracked before they decay, as shown in the left panel of Fig. 5, thus improving the capability to identify weak decays from primary and secondary sources. The resulting expected significance in central (0-10%) Pb-Pb at  $\sqrt{s_{NN}} = 5.52$  TeV as a function of  $p_T$  using standard selections and machine learning is shown in the right panel of Fig. 5.

## 4.3 Heavy-quark correlations

The angular correlation of heavy-flavour hadrons pairs is a powerful probe of QGP scattering, since it is sensitive to the energy loss mechanisms and the degree of thermalization of heavy-quarks in the QGP [7]. The left panel of Fig. 6 shows the ALICE 3 projection for  $D^0 \bar{D}^0$  correlation for minimum-bias Pb-Pb collisions at  $\sqrt{s_{NN}} = 5.52$  TeV. The momentum correlation of heavy-flavour hadron pairs is a powerful probe of the nature of exotic bound states. The nature of recently discovered exotic bound states, like  $T_{cc}^+$  [8], is still unclear. The hypotheses of compact objects like tetraquarks or molecular  $c\bar{c}$  states like  $D^0 D^{*+}$  for  $T_{cc}^+$  are both not excluded. Measurements of the source size dependence of the two-particle momentum correlation function in different colliding systems, from pp to Pb-Pb, provide direct insight into the properties of the  $DD$  interaction potential [9]. The projections for the  $D^0 D^{*+}$  correlation function  $C_{D^0 D^{*+}}$  as a function of the invariant relative momentum  $k^*$  in the hypothesis of the presence of a bound state are shown in the right panel of Fig. 6. These measurements will be out of reach in LHC Runs 3 and 4, since they require excellent pointing resolution, very high identification purity and reconstruction efficiency, as well as large  $\eta$  acceptance, and they will be only possible with ALICE 3.

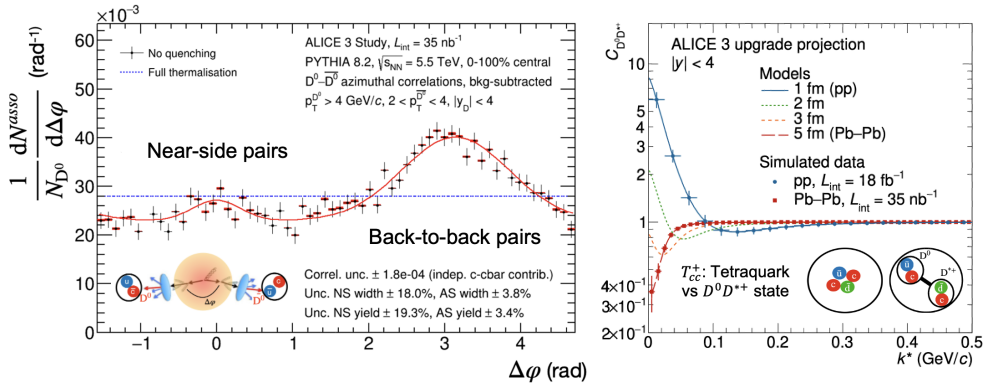


**Figure 6.** Left: Simulated  $D^0\bar{D}^0$  azimuthal correlation distribution in minimum-bias Pb-Pb collisions with ALICE 3 at  $\sqrt{s_{NN}} = 5.52$  TeV. Right: Simulated (dots) and predicted (lines)  $D^0D^{*+}$  correlation  $C_{D^0D^{*+}}$  as a function of the invariant relative momentum  $k^*$  evaluated for different source sizes from pp to Pb-Pb collisions in the hypothesis of the presence of a bound state.

## 5 Conclusions

ALICE 3 is a next-generation multipurpose detector at the LHC, proposed as a follow-up to the present ALICE experiment. Its main goal is to unravel the microscopic dynamics of the QGP produced in heavy-ion collisions and to address fundamental open questions in QCD physics and beyond. An innovative detector concept is required to allow high precision measurements of electromagnetic probes and heavy-flavour hadrons that will remain inaccessible in Runs 3 and 4. Dedicated R&D efforts are ongoing, with significant implications also for future high-energy and nuclear physics experiments.

## References

- [1] ALICE Collaboration, The ALICE experiment: a journey through QCD, *Eur. Phys. J. C* **84**, 813 (2024). <https://doi.org/10.1140/epjc/s10052-024-12935-y>
- [2] Z. Citron et al., Future physics opportunities for high-density QCD at the LHC with heavy-ion and proton beams, CERN-LPCC-2018-07 (2018). <https://cds.cern.ch/record/2650176>
- [3] ALICE Collaboration, Letter of intent for ALICE 3: A next-generation heavy-ion experiment at the LHC, CERN-LHCC-2022-009 (2022). <https://cds.cern.ch/record/2803563>
- [4] R. Rapp, Dilepton Spectroscopy of QCD Matter at Collider Energies, *Advances in High Energy Physics* **2013**, 148253 (2013). <https://doi.org/10.1155/2013/148253>
- [5] P. M. Hohler et al., Is  $\rho$ -meson melting compatible with chiral restoration?, *Physics Letters B* **731**, 103-109 (2014). <https://doi.org/10.1016/j.physletb.2014.02.021>
- [6] A. Andronic et al., The multiple-charm hierarchy in the statistical hadronization model, *J. High Energy Phys.* **2021**, 35 (2021). [https://doi.org/10.1007/JHEP07\(2021\)035](https://doi.org/10.1007/JHEP07(2021)035)
- [7] M. Nahrgang et al., Azimuthal correlations of heavy quarks in Pb + Pb collisions at  $\sqrt{s} = 2.76$  TeV at the CERN Large Hadron Collider, *Phys. Rev. C* **90**, 024907 (2014) <https://doi.org/10.1103/PhysRevC.90.024907>
- [8] LHCb Collaboration. Observation of an exotic narrow doubly charmed tetraquark. *Nat. Phys.* **18**, 751–754 (2022). <https://doi.org/10.1038/s41567-022-01614-y>
- [9] Y. Kamiya et al., A. Femtoscopic study on  $DD^*$  and  $D\bar{D}^*$  interactions for  $T_{cc}$  and  $X(3872)$ . *Eur. Phys. J. A* **58**, 131 (2022). <https://doi.org/10.1140/epja/s10050-022-00782-y>